Date: July 19, 2007
Version: 1.0
Editors: S. Habib, V. Radescu, S. Glazov, E. Rizvi
Referees: P. Laycock, A. Mehta
Comments by

Submitted to
The 2007 Europhysics Conference on High Energy Physics, EPS07, July 19, 2007, Manchester
Abstract: **233**
Parallel Session **Strong Interactions**
Electronic Access: www-h1.desy.de/h1/www/publications/conf/conf_list.html

Measurement of the Inclusive ep Scattering Cross Section at high Q^2 and High y

H1 Collaboration

Abstract

A measurement of the reduced double differential cross section, $\tilde{\sigma}(x, Q^2)$, is presented for the neutral current process, $ep \to eX$, at very high y: $0.63 < y < 0.9$, for intermediate Q^2 in the range 60 to $1,000$ GeV^2. The cross section measurement uses the complete HERA-II data set; a factor three improvement in luminosity over previously published data. The high y cross section is sensitive to the proton structure functions $\tilde{F}_2$ and $\tilde{F}_L$ and thus provides additional constraint on the gluon density of the proton.

1 Introduction

Precision measurements of proton structure in Deep Inelastic Scattering (DIS) are vital to understanding the detailed nature of Quantum Chromo-Dynamics. Previously published measurements [1–4] have already provided unique constraints [1, 4–6] on the parton density functions (PDFs) of the proton. In this paper new measurements of the reduced neutral current cross section, $\tilde{\sigma}(x, Q^2)$, in the region of very high inelasticity, y, and intermediate Q^2 are presented. This kinematic region is of particular importance in providing PDF constraints for QCD evolution from the HERA regime into the phase space probed by central production of massive particles at the LHC experiments.

The measurments use the complete HERA-II data set amounting to the analysis of 315 pb^{-1} of luminosity collected between 2003 and 2007. Of this, 161pb^{-1} is from e^+p collisions and 154pb^{-1} is from e^-p collisions. Both lepton charge samples were collected with approximately equal luminosity between left and right handed longitudinal polarisation of the lepton beams, yielding unpolarised e^+p and e^-p data samples.

The differential cross section for $e^\pm$ scattering after correction for QED radiative effects is given by

$$\frac{\mathrm{d}^2\sigma^\pm_{\mathrm{NC}}}{\mathrm{d}x\mathrm{d}Q^2} = \frac{2\pi\alpha^2}{xQ^4}(Y_+\tilde{F}_2 \mp Y_- x\tilde{F}_3 - y^2\tilde{F}_L) \ . \tag{1}$$

Neglecting the effects of the $x\tilde{F}_3$ structure function (which arises from Z^0 exchange at high Q^2), the reduced cross section is then defined by

$$\tilde{\sigma}^\pm(x, Q^2) \equiv \frac{\mathrm{d}^2\sigma^\pm_{\mathrm{NC}}}{\mathrm{d}x\mathrm{d}Q^2}\frac{xQ^4}{2\pi\alpha^2}\frac{1}{Y_+} \equiv \tilde{F}_2 - \frac{y^2}{Y_+}\tilde{F}_L \ . \tag{2}$$

The helicity dependence of the interactions is contained within the terms $Y_\pm = 1 \pm (1 - y^2)$ where y characterises the inelasticity of the interaction, and is the fractional energy loss of the scattered lepton in the centre of mass frame.

The cross section is dominated by the $\tilde{F}_2$ structure function, but at high y the $\tilde{F}_L$ contribution plays an increasingly significant role. At leading order QCD this contribution is identically zero, but is non-zero at NLO QCD due to the effects of gluon radiation. Thus a direct measurement of $\tilde{F}_L$ provides a direct constraint on the gluon density in the proton.

2 Experimental Technique

The H1 detector components most relevant to this analysis are the liquid argon (LAr) calorimeter, which measures the positions and energies of charged and neutral particles over the polar[1] angular range $4^\circ < \theta < 154^\circ$, and the inner tracking detectors, which measure the angles and

[1]The polar angle θ is defined with respect to the positive z axis, the direction of the incident proton beam.

momenta of charged particles over the range $7^\circ < \theta < 165^\circ$. A full description of the detector can be found in [7].

The ep luminosity is determined by measuring the QED bremsstrahlung ($ep \to ep\gamma$) event rate by tagging the low angle scattered lepton in a detector located at $z = -44$m adjacent to the beam pipe.

Simulated DIS events are used in order to determine acceptance corrections. DIS processes are generated using the DJANGO [8] Monte Carlo (MC) simulation program. In the event generation the DIS cross section is calculated using the H1 PDF 2000 [4] parametrisation for the proton PDFs. The detector response to events produced by the generation programs is simulated in detail using a program based on GEANT [9]. These simulated events are then subjected to the same reconstruction and analysis chain as the data.

NC events are characterised by an isolated high transverse momentum lepton and a hadronic system opposite in azimuth to the scattered lepton. The NC kinematic quantities are determined using the e method which uses the measurement of the scattered lepton energy, E'_e, and polar angle, θ_e to reconstruct the kinematic variables y and Q^2.

$$y = 1 - \frac{E'_e(1 - \cos\theta_e)}{2E_e} \quad Q^2 = \frac{E'^2_e \sin^2\theta_e}{1 - y}$$

At fixed centre-of-mass energy, $\sqrt{s}$, the Bjorken scaling variable x is determined using the relation

$$x = \frac{Q^2}{sy}.$$

At high y this reconstruction method has excellent resolution in both Q^2 and y.

The NC sample is used to carry out an *in-situ* calibration of the electromagnetic and hadronic energy scales of the LAr calorimeter using the method described in [4, 10, 11]. The hadronic final state particles are reconstructed using a combination of tracks and calorimeter deposits in an energy flow algorithm that avoids double counting [10, 11]. The hadronic calibration procedure is based on the double angle reconstruction method [12] which uses the polar angles of the scattered lepton and the hadronic final state to determine their respective energies. The calibration procedure gives good agreement between data and simulation within an estimated uncertainty of 4% on the hadronic scale and 2% on the electromagnetic scale.

The selection of candidate NC events follows closely that of the previously published analysis from H1 [4]. Candidate NC interactions are selected by requiring the scattered lepton energy $E'_e > 5.5\,\mathrm{GeV}$, $890 > Q^2 > 56$ GeV^2 and a reconstructed vertex within $35\,\mathrm{cm}$ in z of the nominal interaction point.

The high y region also corresponds to the kinematic phase space in which the hadronic final state is observed in the central and backward regions of the detector. This, coupled with the low energy of the scattered lepton renders the analysis susceptible to large photoproduction background. Background from misidentified leptons (primarily $\pi^0 \to \gamma\gamma$) is suppressed by requiring a good quality charged track to be associated to the lepton candidate.

Longitudinal energy-momentum conservation requires that $E - P_z = 2E_e$ where E_e is the lepton beam energy and E and P_z are the usual four vector components of the summed hadronic

final state and scattered lepton. The requirement $E - P_z > 35$ GeV suppresses the contamination from photoproduction background in which the the scattered lepton is undetected in the backward beam pipe and a hadron is misidentified as a scattered lepton candidate. In addition this requirement reduces the influence of initial state bremmsstrahlung radiative corrections.

A sizeable background remains after these selection criteria in which a charged track is associated to the fake lepton calorimetric energy deposition. If the background is assumed to be charge symmetric, then events with a wrongly charged track (with respect to the lepton beam charge) provide a good estimate of the remaining background in the sample of events with a correctly charged track. The uncertainty in this statistical background subtraction, using data alone arises, from any possible charge asymmetry in the background and is accurately estimated by comparing the wrong charged candidate events in the e^+p and e^-p data samples.

The region of high y corresponds to the kinematic region of low energy of the scattered lepton. Here, NC events are triggered mainly using information from the LAr calorimeter. The trigger used for this analysis requires a compact electromagnetic energy deposition in the LAr calorimeter. Since the trigger is only fully efficient for lepton energies above 11 GeV a detailed study of the threshold behaviour of the trigger at lower energies down to 5.5 GeV is neccesary. Two samples of independently triggered events are used to determine the efficiency. After removal of inefficient regions of the calorimeter, the efficiency is found to be 50% at 6 GeV and almost 100% efficient for leptons above 11 GeV. This efficiency is well modelled in the MC simulation.

---

3 Control Plots and Systematic Uncertainties

Comparisons of the data and the simulation, are shown in Figs. 1 and 2. In both cases, the solid points show the data events with a correctly charged track, the shaded histogram shows the data with the wrongly charged track, and the full line shows the summed contribution of the MC simulation (with a small contribution from wrongly charged events subtracted) and background from the wrongly charged data. All plots are normalised to the number of candidate events in the data.

Fig. 1 shows the distribution of scattered lepton energy E'_e, the lepton polar angle θ_e, the reconstructed Z position of the interaction vertex Z_v, and the total $E - P_z$ of the scattered lepton and the hadronic final state. The distribution is shown below the cut value of 35 GeV. The shaded histogram shows the contribution of fake events having a wrongly charged track associated to the scattered lepton. In Fig. 2 the kinematic variables y, x and Q^2 for the data. The MC provides an excellent description of the shapes of distributions in the data. In all cases the simulation provides an accurate description of the data.

The selected event samples are corrected for detector acceptance and migrations using the simulation and are converted to bin centered cross sections. The bins used in the measurement are required to have stability and purity[2] larger than 30%

[2]The stability (purity) is defined as the number of simulated events which originate from a bin and which are reconstructed in it, divided by the number of generated (reconstructed) events in that bin.

The systematic uncertainties on the cross section measurements are discussed briefly below (see [10, 11] and references therein for more details). Positive and negative variations of one standard deviation of each error source are found to yield errors which are symmetric to a good approximation.

- A 2% uncertainty on the LAr trigger efficiency is assigned. For the most backward region of the calorimeter, at low energy ($z_{imp} < -110$ cm and $E'_e < 8$GeV) this uncertainty is increased to 6.5%. In addition a 0.5% and a 1% (2% in 2003-4) contribution are considered to account for additional weak trigger conditions independent of the LAr calorimeter. All three contributions are summed quadratically.
- The combined uncertainty of finding an interaction vertex and associating a track to the scattered lepton is estimated to be 2%.
- An uncertainty of 2% for the identification of the scattered lepton is considered. This is estimated using an independent track based electron identification algorithm.
- An uncertainty in the polar angle measurement of the scattered lepton is taken to be 3 mrad.
- An uncertainty of 2% is assigned to the scale of the electromagnetic energy measured in the LAr calorimeter
- An uncertainty of 4% is assigned to the scale of the hadronic energy measured in the detector.
- The photoproduction background is estimated directly from the data using wrongly charged (fake) scattered lepton candidates from the e^+p and e^-p data sets. The asymmetry is found to be less than 2%.
- In addition, there is a global normalisation uncertainty of 4% from the luminosity measurement.

The total systematic error is formed by adding the individual uncertainties in quadrature. For all measurement bins the total uncertainty is 4.5% (excluding the normalisation uncertainty) and is dominated by the systematic error contributions. The largest of these sources of uncertainty arise from the efficiencies of the trigger, the track and event vertex determination, and the scattered lepton identification. It is expected to be able to substantially reduce these sources of uncertainty in the near future.

4 Results

In Fig. 3 the reduced cross section is shown for $y = 0.75$ and for the published HERA-I data based on a luminosity of 65 pb^{-1}. The new measurements show a simlar Q^2 dependence of the cross sections as the published data, and have a tendency to lie systematically higher. The

difference in normalisation between the HERA-I data and the preliminary HERA-II data is within the quoted normalisation uncertainties of 1.5% for HERA-I and 4% for HERA-II.

The new measurements are everywhere systematically limited, and at lower Q^2 have a comparable precision to the published data. At higher Q^2 the new data give a substantial improvement in the precision of the measurement. In addition the new data extend the measurement region to lower Q^2.

5 Conclusions

A new measurement of the reduced double differential cross section $\tilde{\sigma}(x, Q^2)$ is presented for intermediate Q^2 and very high y. This data are sensitive to the $\tilde{F}_L$ structure function and therefore provide an additional constraint on the gluon density of the proton. The new data, limited by systematic uncertainties, give improved precision at high Q^2 over existing measurements, and extend the measurement into a new kinematic region at lower Q^2.

Acknowledgements

We are grateful to the HERA machine group whose outstanding efforts have made this experiment possible. We thank the engineers and technicians for their work in constructing and maintaining the H1 detector, our funding agencies for financial support, the DESY technical staff for continual assistance and the DESY directorate for support and for the hospitality which they extend to the non DESY members of the collaboration.

References

[1] C. Adloff *et al.* [H1 Collaboration], Eur. Phys. J. C **21** (2001) 33 [hep-ex/0012053].

[2] C. Adloff *et al.* [H1 Collaboration], Eur. Phys. J. C **13**, 609 (2000) [arXiv:hep-ex/9908059].

[3] C. Adloff *et al.* [H1 Collaboration], Eur. Phys. J. C **19**, 269 (2001) [arXiv:hep-ex/0012052].

[4] C. Adloff *et al.* [H1 Collaboration], Eur. Phys. J. C **30** (2003) 1 [hep-ex/0304003].

[5] D. Stump, J. Huston, J. Pumplin, W.K. Tung, H.L. Lai, S. Kuhlmann and J.F. Owens, JHEP **0310** (2003) 046 [arXiv:hep-ph/0303013].

[6] A.D. Martin, R. G. Roberts, W. J. Stirling and R. S. Thorne, Phys. Lett. B **604** (2004) 61 [arXiv:hep-ph/0410230].

[7] I. Abt *et al.* [H1 Collaboration], Nucl. Instrum. Meth. A **386** (1997) 310 and 348;
R.D. Appuhn *et al.* [H1 SPACAL Group], Nucl. Instrum. Meth. A **386** (1997) 397.

[8] G.A. Schuler and H. Spiesberger, Proceedings of the Workshop "Physics at HERA", vol. 3, eds. W. Buchmüller, G. Ingelman, DESY (1992) 1419.

[9] R. Brun *et al.*, GEANT3 User's Guide, CERN-DD/EE-84-1 (1987).

[10] B. Portheault, Ph.D. thesis (March 2005), LAL 05-05 (IN2P3/CNRS), Université de Paris-Sud XI, Orsay, available at http://www-h1.desy.de/publications/theses_list.html.

[11] A. Nikiforov, Ph.D. thesis (*in preparation)*, Max-Planck-Institut für Physik, Munich, will be available at http://www-h1.desy.de/publications/theses_list.html.

[12] S. Bentvelsen et.al., Prceedings of the Workshop "Physics at HERA", vol.1, eds. W. Buchmüller, G. Ingelman, DESY (1992) 23; C. Hoeger, ibid, 43.

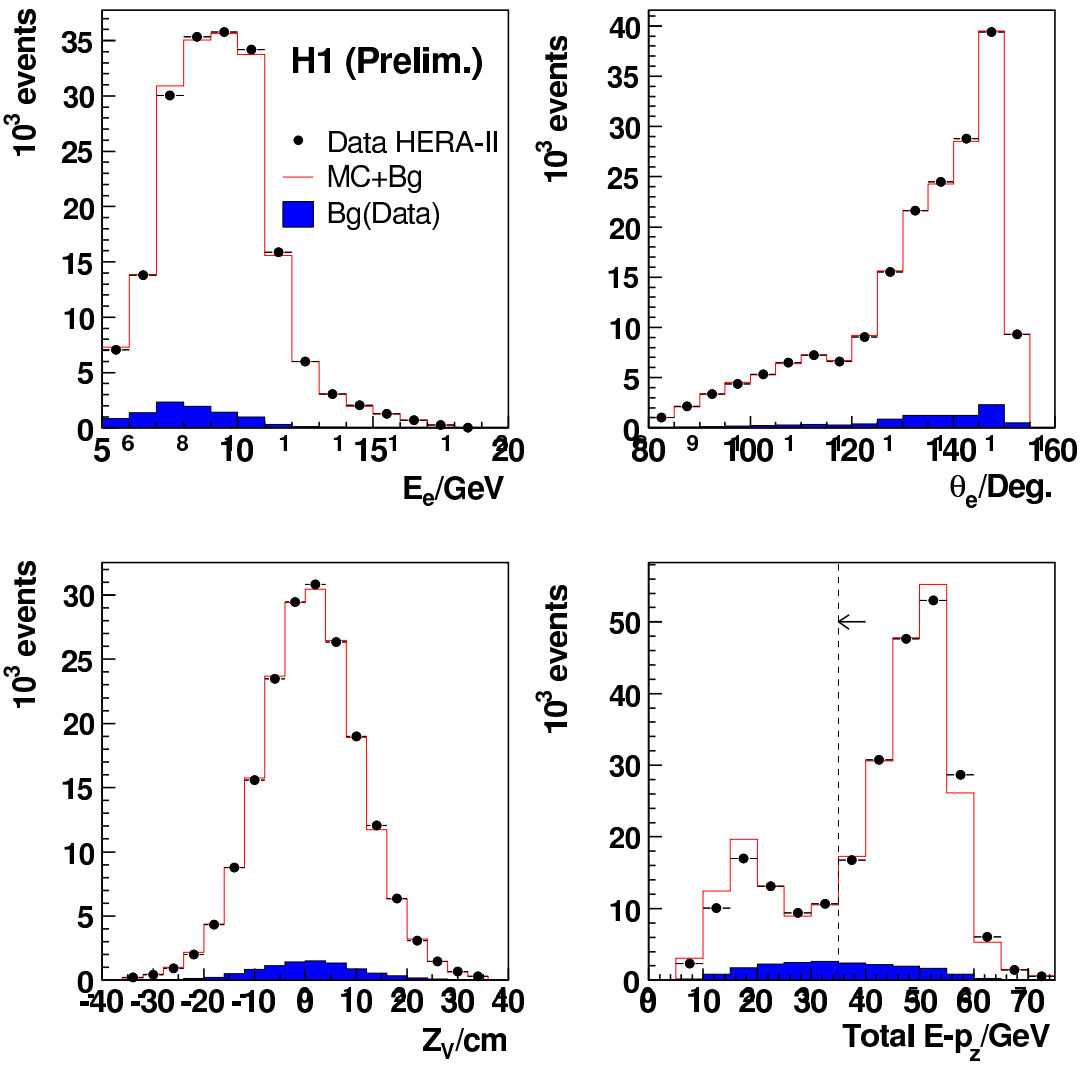

Figure 1: Distributions of the scattered lepton energy, E'_e, and polar angle, θ_e, as well as the z position of the reconstruted interaction vertex, Z_v, and the total event $E - P_z$. The solid points are the correct sign data, the shaded histogram is the wrong sign data and the full line shows the sum of correct sign MC simulation and wrong sign data. The full line is normalised to the number of candidate data events.

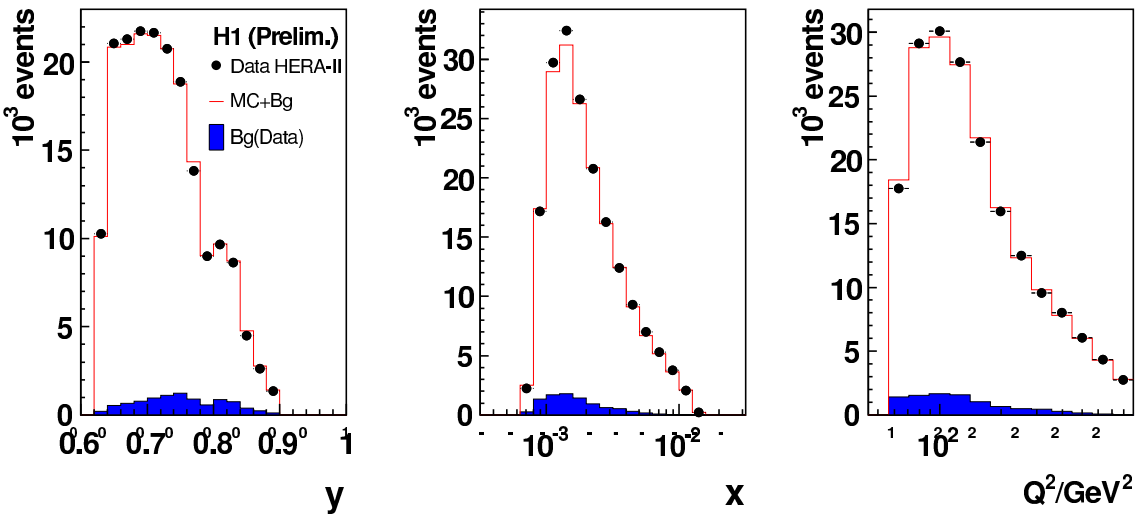

Figure 2: Distributions of the kinematic quantitites, y,x, and Q^2. The solid points are the correct sign data, the shaded histogram is the wrong sign data and the full line shows the sum of correct sign MC simulation and wrong sign data. The full line is normalised to the number of candidate data events.

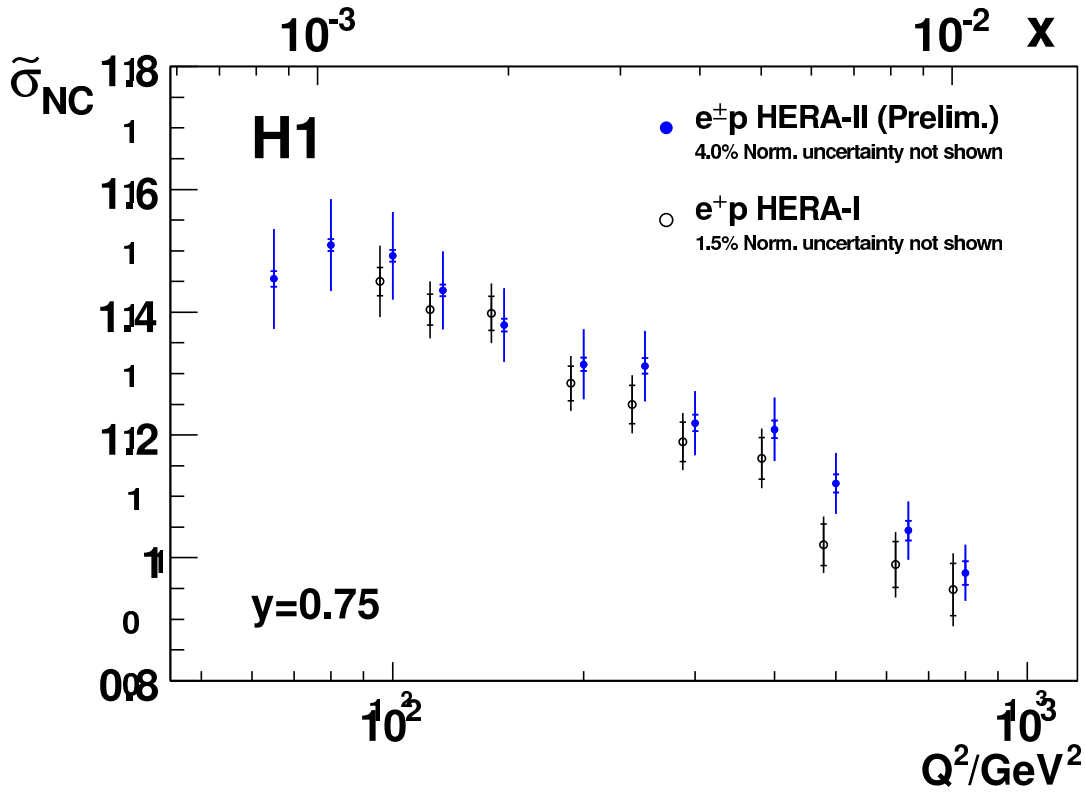

Figure 3: The reduced cross section, $\tilde{\sigma}(x, Q^2)$, is shown as a function of Q^2 (lower scale), or x (upper scale) for fixed $y = 0.75$. The new data presented here are shown in solid points, and are compared the previously published data from the H1 collaboration in open points. The inner error bar represents the statistical uncertainty on the measurement, and the out error represents the total statistical and systematic uncertainty. The normalisation uncertainties are not included in the error bars.